



## Exploring Mechanism of Actions for Eugenol and Beta-Caryophyllene to Combat Colorectal Cancer Chemotherapy Using Network Pharmacology

Krupali Trivedi<sup>1</sup> , Pooja Rathaur<sup>2</sup> , Nilam Parmar<sup>2</sup> , Suraj Pancholi<sup>3</sup> , Brijesh Gelat<sup>1</sup> ,  
 Shiva Chettiar<sup>4</sup> , Alpesh Patel<sup>4</sup> , Devendrasinh Jhala<sup>1\*</sup> 

<sup>1</sup>Department of Zoology, University School of Sciences, Gujarat University, Ahmedabad, Gujarat 380009, INDIA.

<sup>2</sup>Department of Life Science, University School of Sciences, Gujarat University, Ahmedabad, Gujarat 380009, INDIA.

<sup>3</sup>Department of Computer Science, Gujarat University, Ahmedabad, Gujarat 380009, INDIA.

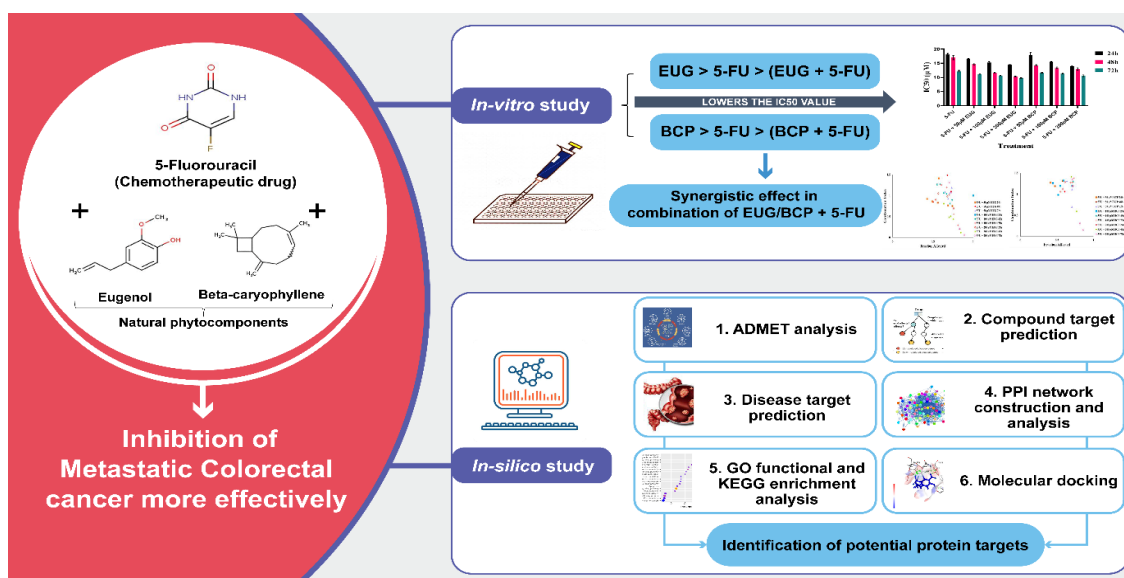
<sup>4</sup>Genexplore Diagnostics and Research Centre Pvt. Ltd., 1201 to 1210, Iconic Shyamal, Shyamal cross road, Satellite, Ahmedabad, Gujarat 380015, INDIA.

Received – February 11, 2024; Revision – April 04, 2024; Accepted – April 23, 2024

Available Online – May 15, 2024

DOI: [http://dx.doi.org/10.18006/2024.12\(2\).188.202](http://dx.doi.org/10.18006/2024.12(2).188.202)

### GRAPHICAL ABSTRACT



\* Corresponding author

E-mail: [ddjhala@gmail.com](mailto:ddjhala@gmail.com) (Devendrasinh Jhala)

Peer review under responsibility of Journal of Experimental Biology and Agricultural Sciences.

Production and Hosting by Horizon Publisher India [HPI]  
 (<http://www.horizonpublisherindia.in/>).  
 All rights reserved.

All the articles published by [Journal of Experimental Biology and Agricultural Sciences](http://www.jebas.org) are licensed under a [Creative Commons Attribution-NonCommercial 4.0 International License](https://creativecommons.org/licenses/by/4.0/) Based on a work at [www.jebas.org](http://www.jebas.org).



## KEYWORDS

Beta-caryophyllene  
 Caspase-3  
 Colorectal cancer  
 Eugenol  
 Multi-targeted approach  
 Synergism

## ABSTRACT

This study explores the potential of essential oils, Eugenol (EUG), and Beta-Caryophyllene (BCP) in enhancing the efficacy of the chemotherapeutic drug 5-fluorouracil (5-FU) in treating metastatic colorectal cancer (CRC). Pharmacokinetic assessment through ADMET analysis indicates that EUG and BCP adhere to the rule of five with good bioavailability, ensuring their drug-likeness properties. The study employs a multitarget strategy to reduce drug dosage and enhance effectiveness, testing the compounds on the HCT116 human colorectal cancer cell line. MTT assay revealed *in-vitro* cytotoxic effects of EUG, BCP, and 5-FU, with a noteworthy reduction in  $IC_{50}$  values observed when combining the compounds, indicating synergistic effects ( $CI < 1$ ) as depicted in the Fa-CI plot. Network pharmacology-based analysis of the compound-disease-target (C-D-T) network identifies 58, 24, and 49 target proteins for EUG, BCP, and 5-FU, respectively, in metastatic CRC. Venn diagram intersection reveals 11 common target proteins, and the merged C-D-T network highlights 84 target proteins, with 16 selected based on edge count, including HSP90AA1, IGF-1R, ESR1, and CASP3. Molecular docking studies indicate that EUG, BCP, and 5-FU effectively inhibit the core target protein HSP90AA1 within the C-D-T network, suggesting their potential as modulators for CRC metastasis. These findings propose a promising approach for developing drugs targeting specific proteins to mitigate metastasis in colorectal cancer.

## 1 Introduction

Colorectal cancer (CRC) poses a significant global health challenge, with projections indicating a 60% increase by 2030, amounting to 2.2 million new cases and 1.1 million deaths (Toiyama et al. 2014; Arnold et al. 2017; Zhu et al. 2018; Benarba and Pandiella 2018; Huang et al. 2020). Current CRC therapies, encompassing surgery, radiotherapy, chemotherapy, and targeted therapy, face limitations, particularly in managing metastatic lesions (Fan et al. 2020). The widely used chemotherapeutic drug 5-Fluorouracil (5-FU) (Figure 1A), despite its efficacy, is hampered by side effects such as leukopenia, which can lead to life-threatening complications and therapy discontinuation (Kadoyama et al. 2011; Casale and Patel 2022).

In pursuit of alternative therapies, this study focuses on natural compounds, specifically eugenol (EUG) (Figure 1B) and beta-caryophyllene (BCP) (Figure 1C), derived from plants like *Eugenia caryophyllata* and *Ocimum sanctum*. Inspired by Hippocrates' wisdom, the research explores the medicinal properties of these compounds, known for their antioxidant, antimicrobial, anticancer, and anti-inflammatory effects (Fernández-Ruiz et al. 2013; Ulanowska and Olas 2021; Alonso Gómez et al. 2022).

Leveraging network pharmacology, the prime aim of the study is to assess the pharmacokinetic properties and interactions of EUG and BCP with core target proteins in CRC. Molecular docking validates these targets, providing insights into the mechanism of action on various cell signaling pathways. This research offers a

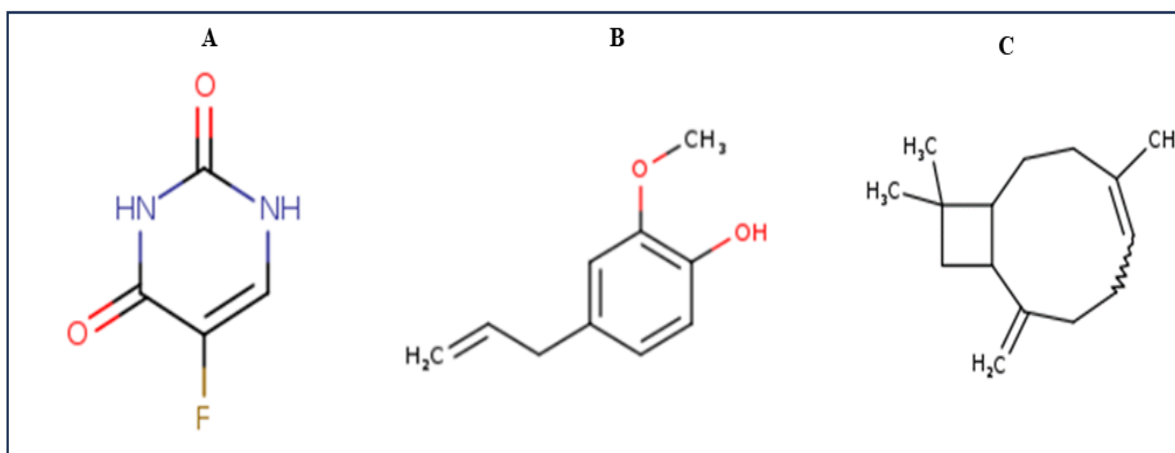


Figure 1 Structures of (a) 5-Fluorouracil (5-FU), (b) Eugenol (EUG), (c) Beta-caryophyllene (BCP)

promising avenue for developing safer and more effective CRC treatments based on natural compounds derived from herbal sources.

## 2 Materials and methods

### 2.1.1 Cell culture and maintenance

Human Colorectal Carcinoma cell line HCT116 was obtained from the National Centre for Cell Science (NCCS), Pune, Maharashtra, India. Cells were cultured in DMEM medium supplemented with 10% FBS, 100 mg/mL streptomycin, and 100 U/mL penicillin and maintained at 37 °C with 5% CO<sub>2</sub>. Cells were sub-cultured on attaining ~ 80% confluency for further experiments using 96 or 24-well plates.

### 2.1.2 MTT (3-(4,5-dimethylthiazol-2-yl)-2, 5-diphenyltetrazolium bromide) assay

Cytotoxicity was measured using an MTT reagent to detect NADH-dependent dehydrogenase activity of the test compounds (Mosmann 1983). Briefly, HCT116 cells were seeded in a 96-well plate at  $5 \times 10^3$  cells/well density, allowed to attach and grow for 24h in a complete DMEM medium, then treated with different concentrations of EUG (1  $\mu$ M to 1000  $\mu$ M), BCP (1  $\mu$ M to 1000  $\mu$ M), and 5-FU (3  $\mu$ M to 1537.53  $\mu$ M). For the combination study, three concentrations of EUG (50  $\mu$ M, 100  $\mu$ M, and 200  $\mu$ M) and BCP (50  $\mu$ M, 100  $\mu$ M, and 200  $\mu$ M) were combined with 5-FU (6  $\mu$ M to 192.19  $\mu$ M) to check their effect on IC<sub>50</sub> value of 5-FU. DMSO was used as vehicle control and maintained 1% in cultures of colorectal cancer cells. After the treatment for 24h, 48h, and 72h with test compounds, the culture medium was removed, followed by PBS wash (pH 7.0), and 50  $\mu$ L MTT reagent (5 mg/mL in PBS) was added into each well and incubated for 4h at 37°C in humidified (5%) CO<sub>2</sub> incubator (Biocenter, Salvis Lab) in dark condition for formazan crystal formation. Afterward, 100  $\mu$ L DMSO was added to solubilize formazan crystals and further incubated for 30 min. MTT product was quantified as absorbance using a microplate reader (Bio-Tek Epoch microplate spectrophotometer, Vermont, USA) at 570nm. Percentage Cell survival was calculated using the formula [mean A570 treated cells – mean A570 blank /mean A570 control cells – mean A570 blank]. IC<sub>50</sub> value was counted using the GraphPad Prism V8.2.1.

### 2.1.3 Estimation of Combination Index (CI)

The CI theorem of Chou-Talalay (Chou and Talalay 1984) quantitatively determines synergism or antagonism at different effect levels as indicated by Fa-CI plot in CompuSyn simulation and automated graphics which were generated for 5-FU-EUG (FE) and 5-FU-BCP (FB) combinations.

## 2.2 Pharmacokinetic assessment

Pharmacokinetic and pharmacodynamic studies of EUG, BCP, and 5-FU, such as absorption, distribution, metabolism, and excretion (ADME) were carried out for drug-likeness properties and toxicity. Other pharmacologically acceptable properties, such as molecular weight, solubility, hydrogen bond acceptor and donor, rotatable bonds, etc., were performed using PreADMET (<https://preadmet.bmdrc.kr>) and SwissADME ([www.swissadme.ch](http://www.swissadme.ch)). SDF (Structure Data File) and SMILES (simplified molecular input line entry system) strings were employed throughout the process. The results were analyzed and compared for each test compound and drug.

## 2.3 Compound targets prediction

3D structure of EUG, BCP, and 5-FU were downloaded in SDF (Structure Data File) format from PubChem (<https://pubchem.ncbi.nlm.nih.gov/>), which were deposited to find Potential targets for all three compounds into PharmMapper (<http://www.lilab-ecust.cn/pharmmapper/>), ChEMBL (<https://www.ebi.ac.uk/chembl/>) and Search Tool for Interacting Chemicals (STITCH) version 5.0 (<http://stitch.embl.de/>) database. Protein-compound interactions were analyzed at 0.900 (Highest) confidence level for *Homo sapiens* species only. We combined all the protein targets to make a common list of targets for each compound.

## 2.4 Acquisition of disease-associated target genes

DisGeNET (<https://www.disgenet.org/>) and Pathcards (<https://pathcards.genecards.org/>) were used to identify proteins related to metastatic Colorectal cancer (Disease ID: C0009402), in which genes  $\geq 0.1$  score gda (Gene Disease Association) were selected for further study. Together, we clubbed both lists of genes together to make a standard list of proteins involved in metastatic CRC.

## 2.5 Protein-Protein interaction (PPI) network formation

PPI networks provide a valuable framework of proteins for understanding functional proteomes in much better ways. That was done using String (<https://string-db.org/>, ver 11.5), with organisms limited to *Homo sapiens* only. PPI with the highest confidence scores ( $> 0.9$ ) were reserved for this study.

## 2.6 Compound-Disease-Target (C-D-T) network construction and analysis

Network constructed using Cytoscape 3.9.1 software. The EUG, BCP, 5-FU PPI networks were merged with the metastatic CRC network using the "Merge" tool of Cytoscape (intersection and union options were selected) to construct the C-D-T network. We

removed duplicated edges and self-loops to present the final network. Node degree was assessed for each network using the Network Analyzer version 4.4.6 plugin (Assenov et al. 2008). The Tanimoto coefficient was calculated to compare the similarity between 5-FU and test substances using the ChemMine tool (<https://chemminetools.ucr.edu/>). The value of the Tanimoto coefficient falls between 0 and 1, and its higher values indicate a greater resemblance than the lower ones.

## 2.7 Enrichment analysis for key targets

DAVID (The Database for Annotation, Visualization, and Integration Discovery) version 8.0.0 was used for GO (Gene Ontology) and KEGG (Kyoto Encyclopaedia of Genes and Genomes) pathway enrichment analysis of EUG, BCP, and 5-FU involved in metastatic CRC to explore their functional role in the human body like Biological Processes (BP), Cellular Compounds (CC), and Molecular Functions (MF) as well as different cell signaling pathways connected to them.

## 2.8 Extracting core targets of the network

With the aid of Microsoft Excel, we intersected the potential target database related to compounds and the target database to get the core target associated with CRC, which was used to draw a Venn diagram online (<http://www.bioinformatics.com.cn/>). Protein targets from the intersected network and the top 16 proteins from a merged network of all three compounds with CRC were taken for further validation using molecular docking.

## 2.9 Molecular docking

Molecular docking was performed using Glide version 11.8 (Halgren et al. 2004). High-resolution protein crystalline structures were obtained by the X-ray diffraction method and presented resolutions smaller than 2.8 Å (Table 8) and were downloaded from the Research Collaboratory for Structural Bioinformatics protein databank (<https://www.rcsb.org/>) and prepared using protein preparation wizard tool (Schrödinger, LLC). Water and hetero molecules were removed, hydrogen atoms were added to the protein structure, optimized, and minimized by inducing potential ionization at pH 7.0 ± 2.0. Restrained minimization was defaulted at 0.30 Å coverage heavy atoms to RMSD value. The receptor grid was generated at the protein's active pocket site, the native ligand called an inhibitor or positive control. Ligand structures for EUG, BCP, 5-FU, and all positive controls were downloaded from PubChem in SDF format prepared with the Ligprep tool (Schrödinger, LLC). Molecular docking was performed at the extra precision (XP) mode for all tested compounds. The final evaluation of ligand-protein binding was performed based on glide score (Kcal/mol). The Discovery Studio program was also used for visual inspection and graphical representations of the docking results.

## 2.10 Statistical analysis

The results were expressed as Mean ± SD analyzed with two-way analysis of variance (ANOVA) for IC<sub>50</sub> values using GraphPad Prism 8.2.1. Further,  $P < 0.05$  was considered to be significantly different. Dunnett's multiple comparison test was performed to compare the IC<sub>50</sub> value of the combination group with the 5-Fluorouracil alone group to test the reduction in inhibitory effect.

## 3 Results and discussion

### 3.1 MTT assay and CI prediction

MTT assay was used to assess the antiproliferative effect of 5-Fluorouracil (5-FU), Eugenol (EUG), and Beta-caryophyllene (BCP) against colorectal cancer (CRC) cell line HCT116 with different concentration at 24h, 48h, and 72h. The inhibitory effects are presented in figure 2 (A, B, C), which indicated dose and time-dependent decrease in the percentage cell survival of CRC cells. The inhibitory concentration (IC<sub>50</sub>) values are shown in table 1. Many researchers have reported anticancer and anti-metastatic properties for all three compounds (Ahmed et al. 2022; Jubeen et al. 2022; Surducan et al. 2023). 5-FU is the most used chemotherapeutic drug in various kinds of cancer, especially colorectal cancer. Due to the narrow therapeutic window, selecting the appropriate dosage is important to avoid the problem of tumor heterogeneity and drug resistance (Kamal et al. 2020; Naren et al. 2022). We aimed to lower the IC<sub>50</sub> value of 5-FU (6 to 192.19 μM) by combining it with the three concentrations of EUG and BCP (50 μM, 100 μM, and 200 μM) to reduce its side effects (Figure 2 D, E). Alone, 5-FU treatment, when compared with its co-treatment of EUG and BCP, has shown a reduction in its IC<sub>50</sub> values by 1.98 for 50 μM EUG to 2.28-fold for 200 μM EUG and 1.83 for 50 μM BCP to 2.34 fold for 200 μM BCP after 24h. Similarly, 1.33 for 50 μM EUG to 1.89 fold for 200 μM EUG and 1.36 for 50 μM BCP to 1.5 fold for 200 μM BCP after 48h. Likewise, 1.58 for 50 μM EUG to 1.81 fold 200 μM EUG and 1.53 for 50 μM BCP to 1.68 fold for 200 μM BCP after 72h treatment, respectively (Table 1). A combination index of less than 1 indicated synergism for combining two drugs. Figure 2 (left and right panel) shows a Fa-CI plot for a combination index lower than 1 when fractions affected (Fa, Percent inhibition of cell survival) were found to be in range of 0.42 to 1.0 for FE and 0.41 to 0.85 for FB in HCT116. 200 μM concentrations of EUG and BCP gave best results at 48h and 72h in combinations. Ng et al. (2014) reported that *Piper betle* leaf extract which contains eugenol as major component enhances the effect of 5-FU in colorectal cancer when given in combination with 4-allylpyrocatechol and *P. betle* crude extract treatment (Ng et al. 2014). As per the previous report of Hemaiswarya and Doble (2013), the combination of eugenol and 5-FU showed synergistic effects against Human cervical cancer (HeLa) cells after 24h treatment. The recent study conducted by Bhardwaj and Dilbaghi in

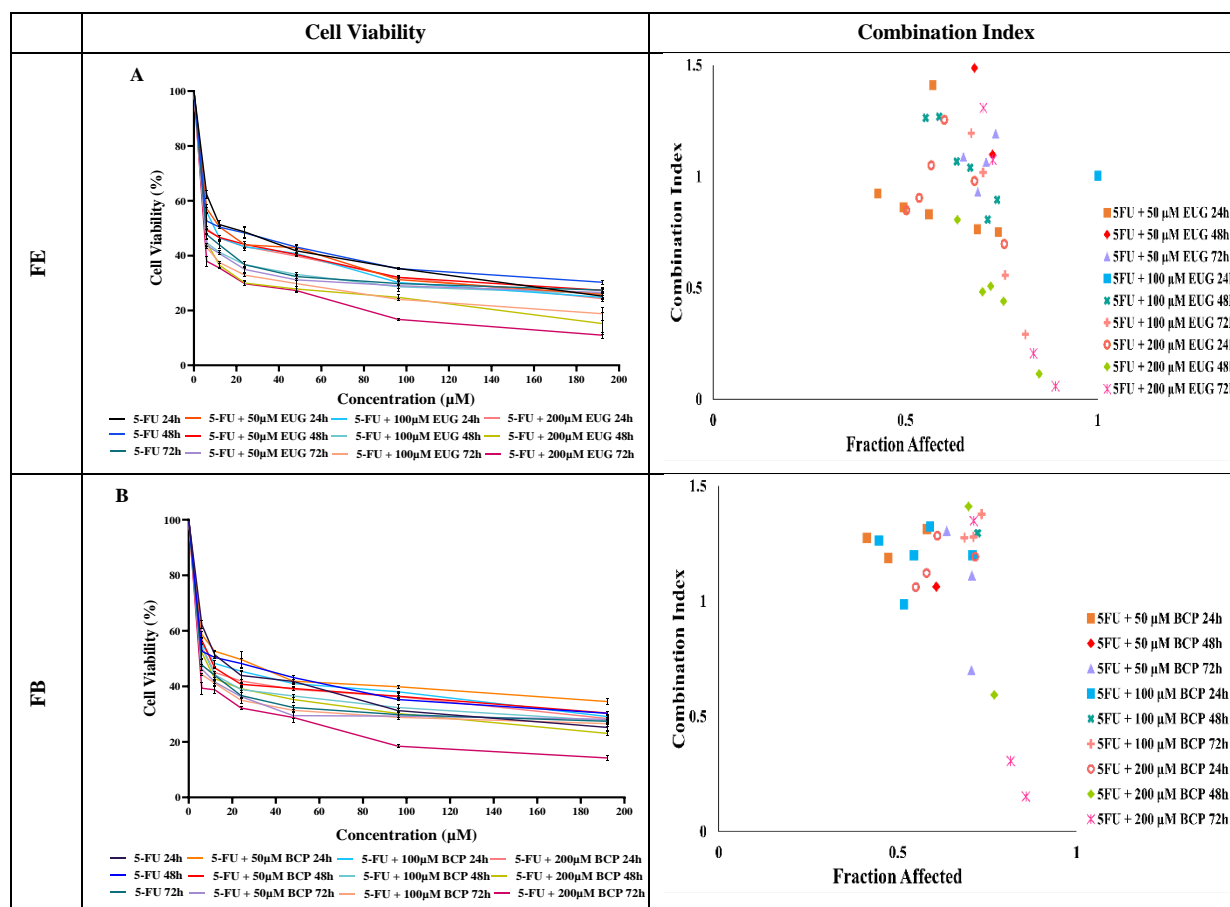
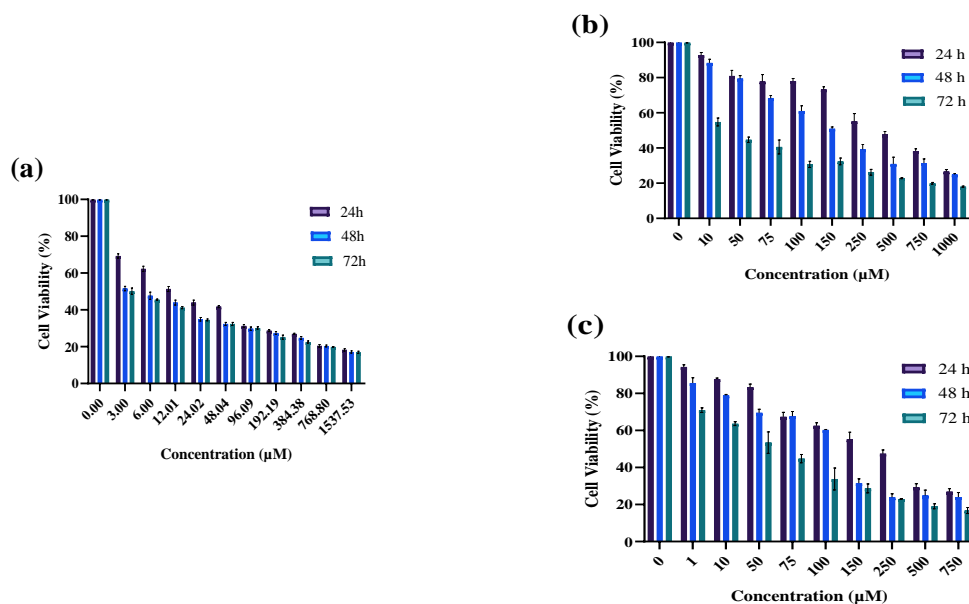


Figure 2 Effect of (A) 5-FU (B) EUG and (C) BCP; 5-Fluorouracil (5-FU) in combination with Eugenol (FE) and 5-Fluorouracil (5-FU) in combination with Beta-caryophyllene (FB) on % Survival (Left panel), Combination Index (Right panel) represented as Combination Index (CI) vs Fraction Affected (Fa) plot of HCT116 Colorectal cancer cells after treatment for 24h, 48h and 72h. Data was represented as Mean  $\pm$  SD for three individual experiments.

Table 1 The inhibitory concentration 50 (IC<sub>50</sub>) values of 5-Fluorouracil (5-FU), Eugenol (EUG), and Beta-Caryophyllene (BCP) alone and Combination of 5-FU and EUG (FE) as well as 5-FU and BCP (FB) for 24h, 48h and 72h in HCT116 cell line

Treatment Group	IC <sub>50</sub> (μM)		
	24h	48h	72h
5-FU	32.92 ± 0.63	19.54 ± 0.77	17.74 ± 0.59
EUG	439.62 ± 2.57	152.64 ± 5.86	56.51 ± 0.75
BCP	202.98 ± 12.18	115.82 ± 3.26	53.11 ± 3.49
5FU + 50 μM EUG	16.61 ± 0.19****	14.67 ± 0.35****	11.20 ± 0.09**
5FU + 100 μM EUG	15.35 ± 0.31****	11.71 ± 0.12****	10.63 ± 0.04****
5FU + 200 μM EUG	14.40 ± 0.14****	10.29 ± 0.11****	9.77 ± 0.12****
5FU + 50 μM BCP	17.98 ± 0.79 <sup>ns</sup>	14.34 ± 0.21****	11.59 ± 0.12 <sup>ns</sup>
5FU + 100 μM BCP	15.51 ± 0.23****	13.37 ± 0.37****	11.31 ± 0.19*
5FU + 200 μM BCP	14.02 ± 0.19****	13.02 ± 0.43****	10.50 ± 0.39****

Results are represented as Mean ± SD; \*\*\*\*P < 0.0001, \*\*P < 0.01, \*P < 0.1, ns=nonsignificant, when 5-FU alone treated group was compared with the combination (5-FU + EUG/ BCP) groups

2022 showed the enhanced cytotoxic potential of 5-FU against the A431 skin cancer cell line by INV-FU (Beta-caryophyllene constellated 5-FU nanoinvasomes) (Bhardwaj and Dilbaghi 2022). The current experiment lowered the IC<sub>50</sub> values of 5-FU by showing the synergistic effect of EUG and BCP in combination with 5-FU.

### 3.2 Evaluation of pharmacokinetic, ADME, and toxicity profile of EUG, BCP, and 5-FU

Evaluating compounds based on their ADME/Tox properties by computational approach has become an elemental segment in drug discovery. Orally administered drugs follow the rule of five or Lipinski's rule, according to which smaller molecules (MW < 500 g/mol) with lipophilic properties (Octanol- water partition coefficient, AlogP98) and ≤5 Hydrogen bond donor as well as acceptor are permeable across membrane bi-layer (Lipinski et al. 1997). According to Veber et al. (2002), the number of rotatable bonds and the topological polar surface area should be within limits (Veber et al. 2002), as given in Table 2 for membrane permeability. A suitable drug-like profile has been found for all

three substances according to the MDDR-like rule (Sheridan and Shpungin 2004). All three bioactive compounds fully comply with this rule and have high bioavailability.

Table 3 shows the ADME properties of EUG, BCP, and 5-FU. The drugs administered should now be able to get absorbed by intestinal cells to exert their effect by reaching target molecules. It is worth mentioning that EUG and BCP have greater HIA (Human Intestinal Absorption) (~100%), Caco, and MDCK cell permeability than 5-FU drugs. They can even cross the Blood-Brain Barrier (BBB) more effectively by binding with plasma proteins than 5-FU, justifying possible plasma transport mechanisms. Further, P-gp (p-glycoproteins) are membrane transporters that efflux the drug when taken in large amounts or quickly absorbed. P-gp inhibitors are present in BBB and other organs, making it even more difficult for the drug to efflux after absorption (Amin 2013). Cytochrome P450 enzyme family, especially CYP2D6, is important for drug metabolism due to its substrate specificity. Inhibitors of this enzyme may lead to drug elevation in the circulatory system and thus increase toxicity levels (Gibbs et al. 2006; Di 2017; Gonzalez et al. 2021). All

Table 2 Evaluation of pharmacokinetic properties of 5-FU, EUG, and BCP

Compound	Lipinski's rule <sup>a</sup>			Veber's rule <sup>b</sup>			MDDR like rule <sup>c</sup>
	MW	AlogP98	HBD	HBA	RBN	TPSA	
5-FU	130.08	-0.62	2	4	0	58.20	Non-druglike
EUG	164.20	2.55	1	2	3	29.46	Mid-structure
BCP	204.35	4.29	0	0	0	00.00	Mid-structure
Optimal	≤500	≤5	≤5	≤10	≤3	7-200	-

<sup>a</sup>MW= Molecular Weight(g/mol), AlogP98= Predicted water/octanol partition coefficient, HBD= Hydrogen Bond Donor, HBA= Hydrogen Bond Acceptor; <sup>b</sup>RBN= Rotatable Bond Numbers, TPSA= Topological Polar Surface Area (Å<sup>2</sup>); <sup>c</sup>MDDR= MDL Drug Data Report

Table 3 *In silico* ADME prediction for 5-FU, EUG, and BCP

Compound	Absorption <sup>a</sup>			Distribution <sup>b</sup>			Metabolism <sup>c</sup>
	HIA	QPPCaCo	QPPMDCK	PPB	Pgp binding	BBB	ADMET CYP2D6 inhibition
5-FU	76.93	16.59	0.95	8.3	No	0.28	No
EUG	96.77	46.88	342.14	100.0	No	2.25	No
BCP	100.00	23.63	45.74	100.0	Inhibitor	11.65	No
Range	70-100, well absorbed	4-70, mid permeability	4-70, mid permeability	>90, strong binding	-	-3-12, permeability to CNS	-

<sup>a</sup>HIA= Human Intestinal Absorption (%), QPPCaCo= in vitro Caco-2 cell permeability (nm/s), QPPMDCK= in vitro MDCK cell permeability (nm/s), <sup>b</sup>PPB= Plasma Protein Binding (%), Pgp binding= P-glycoprotein binding, BBB= in vivo Blood-Brain Barrier penetration (Cbrain/Cblood), <sup>c</sup>ADMET CYP2D6 binding= Cytochrome P450 2D6 binding

Table 4 *In silico* toxicity prediction for 5-FU, EUG, and BCP

Compound	Toxicity prediction				
	Ames_test	Carcino_mouse	hERG_inhibition	TA100	TA1535
5-FU	Mutagen	Positive	Medium risk	Positive	Positive
EUG	Mutagen	Positive	Medium risk	Positive	Positive
BCP	Mutagen	Positive	Medium risk	Positive	Positive

hERG: The human Ether-à-go-go-Related Gene, TA100 and TA1535: *Salmonella typhimurium* strains

three compounds under study do not show binding or inhibition of CYP2D6, hence having good absorbance and efficient metabolism.

*In silico* toxicity tests predicted similar toxicity results in the Ames test for the three compounds (Table 4). For TA100 and TA1535 strains of *Salmonella typhimurium* that are frequently used in the Ames test containing the same base pair replacement mutation hisG4673-75 (Prival and Zeiger 1998; das Chagas Pereira de Andrade and Mendes 2020), EUG and BCP exhibit 5-FU-like behaviour. The model predicted positive carcinogenicity results for EUG, BCP, and 5-FU in both rats and mice. All the substances here show a medium risk for hERG gene inhibition, which encodes the voltage-gated potassium channels in the heart, which is involved in the repolarization process in the heart (Garrido et al. 2020). The results indicate the insured use of EUG and BCP compared to the 5-FU analysis. The substances exhibit many toxicological similarities.

### 3.3 Network Pharmacology Study

Network pharmacology is a modern approach to disease mechanisms targeted by multiple synergistic compounds for drug discovery that define complex drug-disease-gene interactions (Noor et al. 2022). From 5474 genes for metastatic colorectal cancer, 1207 genes were extracted from the DisGeNet based on score-gda  $\geq 0.1$ , which were added to the 116 genes taken from

pathcards. From 1307 unique genes, 761 genes were selected for generating a disease network after eliminating duplicated genes in the Cytoscape app. Whereas 173, 91, and 139 potential genes/proteins were selected after removing duplicated or self-loops from PharmMapper, ChEMBL, STITCH for EUG, BCP, and 5-FU, respectively, to create a network in the Cytoscape app. These identified targets were imported to Cytoscape to generate a Compound-Disease-Target (C-D-T) network. The resultant C-D-T network had 59 nodes/228 edges, 25 nodes/98 edges, and 50 nodes/190 edges against metastatic CRC for EUG, BCP, and 5-FU, respectively (Figure 3A, B, C). This indicates that EUG, BCP, and 5-FU target 58, 24, and 49 proteins of metastatic CRC, excluding the compound node from the network.

Further, by using this app's "Merge" tool, 84 potential gene nodes with 407 edges were found to be the target of all three substances for metastatic CRC. In contrast, the intersection of bioactive compounds and disease showed 11 gene nodes with 25 edges, confirmed by developing a Venn diagram (Figure 3D). The nodes with high edge count/ Node degree were taken as core targets (Table 5) because targeting one protein from the network can connectively disrupt the entire protein network, thus regulating the pathway in cancer. The first 16 common proteins were considered for further validation of the study. The first 15 proteins were present in both merged and intersected analyzed networks of CRC with all three compounds, and one protein, CHEK1, was present in the intersected network.

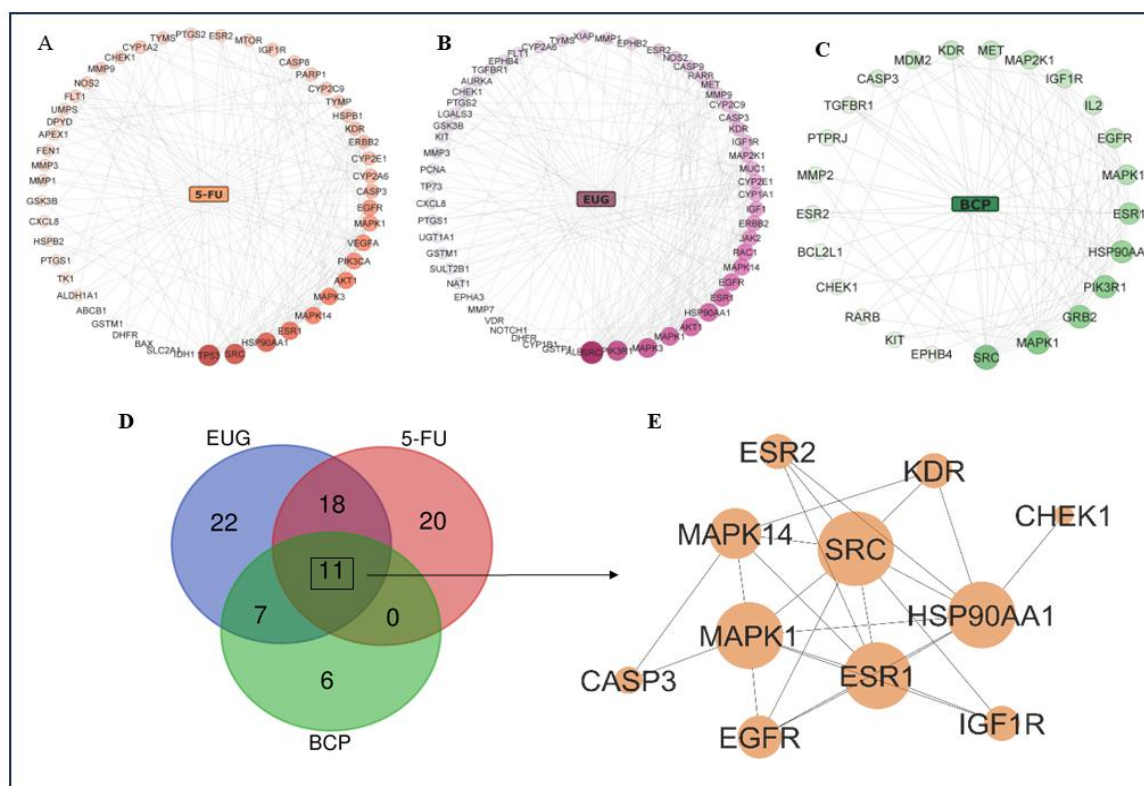


Figure 3 Compound-Disease-Target (C-D-T) network of 5-FU and Test compounds, (A) Node degree sorted C-D-T network of 5-Fluorouracil (5-FU), (B) Eugenol (EUG), (C) Beta-caryophyllene (BCP) against metastatic colorectal cancer (CRC), (D) Venn diagram of intersected hub proteins from 5-FU, EUG and BCP, (E) Protein-Protein interaction (PPI) network of 11 intersected proteins from 5-FU, EUG and BCP against metastatic colorectal cancer (CRC)

Table 5 Potential targets related to CRC with 5-FU, EUG, and BCP merged network

No.	Gene name	Protein name	UniProt ID	Edge count (Node Degree)
1	SRC	proto-oncogene tyrosine-protein kinase Src	P12931	33
2	HSP90AA1	Heat shock protein HSP 90-alpha	P07990	26
3	MAPK1	MAP kinase ERK2	P28482	23
4	ESR1	Estrogen receptor alpha	P03372	23
5	PIK3R1	Phosphatidylinositol 3-kinase regulatory subunit alpha	P27986	22
6	MAPK3	Mitogen-activated protein kinase 3	P27361	21
7	AKT1	RAC-alpha serine/threonine-protein kinase	P31749	21
8	TP53	Cellular tumor antigen p53	P04637	21
9	EGFR	Epidermal growth factor receptor	P00533	21
10	MAPK14	MAP kinase p38 alpha	Q16539	20
11	ERBB2	Receptor tyrosine-protein kinase erbB-2	P04626	14
12	KDR	Vascular endothelial growth factor receptor 2	P35968	14
13	CASP3	Caspase- 3	P42574	14
14	RAC1	Ras-related C3 botulinum toxin substrate 1	P63000	13
15	IGF1R	Insulin-like growth factor I receptor	P08069	13
16	CHEK1	Serine/threonine-protein kinase Chk1	O14757	9

Table 6 Gene ontology (GO) enrichment analysis of the biological process and cellular components, Molecular function for the potential metastatic colorectal cancer (CRC) targets of 5-FU, EUG, and BCP

GO term	Description	5-FU		EUG		BCP	
		GC value	<i>p</i> -value	GC value	<i>p</i> -value	GC value	<i>p</i> -value
Biological Processes (BP)							
GO:0043066	Apoptotic process	11	4.72e <sup>-07</sup>	15	2.30351e <sup>-10</sup>	10	3.99736e <sup>-09</sup>
GO:0030335	Cell migration	7	4.12e <sup>-05</sup>	14	4.63987e <sup>-13</sup>	8	1.43202e <sup>-08</sup>
GO:0008284	Cell proliferation	7	0.002072537	10	2.596e <sup>-05</sup>	8	2.09099e <sup>-06</sup>
GO:0043410	MAPK cascade	5	0.000669133	9	2.20835e <sup>-08</sup>	5	3.57774e <sup>-05</sup>
GO:0035556	Intracellular signal transduction	10	1.34e <sup>-06</sup>	13	5.70211e <sup>-09</sup>	6	0.000155802
GO:0070371	ERK1 and ERK2 cascade	3	0.004080212	5	4.8205e <sup>-06</sup>	3	0.000944176
GO:0042060	Wound healing	4	0.002013155	5	0.000223302	3	0.006354559
Cellular Components (CC)							
GO:0005886	Plasma membrane	12	0.031705895	27	0.000461406	17	7.31094e <sup>-06</sup>
GO:0005634	Nucleus	25	0.001722577	34	4.96908e <sup>-06</sup>	17	6.60645e <sup>-05</sup>
GO:0005737	Cytoplasm	34	1.33e <sup>-09</sup>	32	8.33057e <sup>-06</sup>	14	0.002336449
GO:0005739	Mitochondrion	17	7.95e <sup>-08</sup>	14	0.000121741	8	0.00072934
GO:0005576	Extracellular region	10	0.059458	18	4.892e <sup>-05</sup>	8	0.007481112
GO:0005925	Focal adhesion	6	0.003205	8	0.000179501	4	0.01181298
Molecular Function (MF)							
GO:0005515	Protein binding	41	0.008201	48	0.006371445	23	0.00112074
GO:0004712	Protein serine/threonine/tyrosine kinase activity	11	1.08e <sup>-07</sup>	17	1.07438e <sup>-13</sup>	9	2.58365e <sup>-08</sup>
GO:0003677	DNA binding	-	-	8	0.091920433	5	0.067743477
GO:0004708	MAP kinase kinase activity	3	0.000955	4	2.09929e <sup>-05</sup>	3	0.000217262

GC = Gene Count; *p*-value = Modified Fisher exact *p*-value (EASE score), the smallest, the more enriched.

Cancer is a disease that affects multiple genes, so rather than using single-target drugs, synergistic multiple medicines can act on the same or different multiple proteins to combat the disease (Li et al. 2020). For that, the tanimoto coefficient (value ranges from 0 to 1) was calculated for each bioactive compound to evaluate structural similarity with 5-FU drug, which was found to be 0.06 and 0.007 for EUG and BCP respectively, suggesting that they have the least similarity with 5-FU and can bind with same or different proteins.

### 3.4 Gene Ontology and Kyoto Encyclopaedia of Genes and Genomes Enrichment Analysis

The results of GO analysis (at *p* < 0.05 statistics) (Table 6) showed that all the substances under study targets affected many biological processes such as negative regulation of apoptosis, intracellular

signal induction, MAPK cascade positive regulation, etc. The GO and CC annotations analysis identified various cellular components such as plasma membrane, nucleus, cytoplasm, mitochondria, etc., targeted by 5-FU, EUG, and BCP. It regulates cellular activities through protein binding, DNA binding, and protein serine/threonine/tyrosine kinase activity. KEGG pathway enrichment analysis showed that EUG, BCP, and 5-FU target many cancer cell signaling pathways such as PI3K-Akt, MAPK, VEGF, apoptosis, etc. Among all three compounds, EUG has targeted more pathways genes than the other two, suggesting its potential use in therapeutics (Table 7). An *in vitro* study of eugenol on MDA-MB-231 and SK-BR-3 breast cancer cells revealed its apoptosis-inducing effect via the PI3K-Akt pathway (Abdullah et al. 2021). An experiment on RAW264.7 showed its impact on the down-regulation of NF-κB and MAPK pathways (Deepak et al. 2015).

Table 7 Kyoto Encyclopedia of Genes and Genomes (KEGG) pathway enrichment analysis for the potential metastatic colorectal cancer (CRC) targets of 5-FU, EUG, and BCP

GO term	Description	5-FU		EUG		BCP	
		GC value	<i>p</i> -value	GC value	<i>p</i> -value	GC value	<i>p</i> -value
hsa05200	Pathways in cancer	24	2.21e <sup>-15</sup>	30	1.34646e <sup>-20</sup>	18	3.73925e <sup>-16</sup>
hsa05210	Colorectal cancer	10	1.28e <sup>-09</sup>	11	2.0099e <sup>-10</sup>	7	1.01772e <sup>-07</sup>
hsa04151	PI3K-Akt signaling pathway	14	7.72e <sup>-08</sup>	18	7.29806e <sup>-11</sup>	13	3.33315e <sup>-11</sup>
hsa04010	MAPK signaling pathway	13	8.54e <sup>-08</sup>	16	5.24339e <sup>-10</sup>	11	2.44254e <sup>-09</sup>
hsa04014	Ras signaling pathway	9	5.43e <sup>-05</sup>	13	3.2006e <sup>-08</sup>	10	6.12424e <sup>-09</sup>
hsa04370	VEGF signaling pathway	10	3.93e <sup>-11</sup>	11	4.08898e <sup>-12</sup>	6	5.11946e <sup>-07</sup>
hsa04150	mTOR signaling pathway	7	0.000284	8	7.77016e <sup>-05</sup>	5	0.000864245
hsa01521	EGFR tyrosine kinase inhibitor resistance	13	1.54e <sup>-14</sup>	14	2.58313e <sup>-15</sup>	10	3.49599e <sup>-13</sup>
hsa04210	Apoptosis	9	1.06e <sup>-06</sup>	8	3.23258e <sup>-05</sup>	5	0.000515328

GC= Gene Count; *p*-value = Modified Fisher exact *p*-value (EASE score), the smallest, the more enriched

Table 8 Docking energy score for 5-FU, EUG, and BCP for core protein targets of Compound-Disease-Target (C-D-T) network of metastatic colorectal cancer (CRC) using Glide (XP) program

Name	Target protein		Energy Score (Kcal/mol)			
	PDB ID	Resolution (Å)	5-FU	EUG	BCP	Positive Control
SRC	2BDF	2.10	-5.439	-6.341	-1.898	-9.446
HSP90AA1	4BQG	1.90	-5.097	-7.515	-7.539	-7.853
MAPK1	1WZY	2.5	-3.704	-5.379	-3.594	-10.972
ESR1	5FQV	1.74	-5.028	-5.202	-7.751	-6.78
PIK3R1	3HHM	2.8	-6.015	-4.884	-5.137	-7.598
MAPK3	2ZOQ	2.3	-6.761	-6.018	-2.472	-9.638
AKT1	6CCY	2.18	-6.979	-5.504	-2.617	-8.247
TP53	5O1F	1.38	-3.869	-5.006	-	-6.975
EGFR	4WKQ	1.85	-4.821	-5.752	-3.124	-7.809
MAPK14	6SFO	1.75	-6.283	-7.628	-4.518	-13.469
ERBB2	3PPO	2.25	-5.329	-6.304	-2.194	-14.101
KDR	3WZD	1.57	-4.15	-4.871	-3.829	-10.672
CASP3	1NME	1.60	-4.492	-3.946	-1.884	-5.627
RAC1	3TH5	2.30	-5.324	-6.018	-2.472	-9.638
IGF1R	2OJ9	2.00	-5.112	-6.807	-4.953	-7.442
CHEK1	4QYE	2.05	-5.682	-5.681	-1.473	-9.868

### 3.5 Multitarget Molecular Docking Investigation

This method has been used to assess the interaction between various therapeutic targets of colorectal cancer with our chosen bioactive compounds, eugenol (EUG) and beta-caryophyllene (BCP), as well as standard drug 5-Fluorouracil (5-FU). Sixteen hub

proteins were selected for simulation and were present in all three C-D-T networks of the compounds. The result's binding energy score (Kcal/mol) was negative for all the proteins and ligands, as shown in Table 8. The difference between the energy score of the bioactive component and the respective protein inhibitor was considered the best binding. The lowest difference between positive

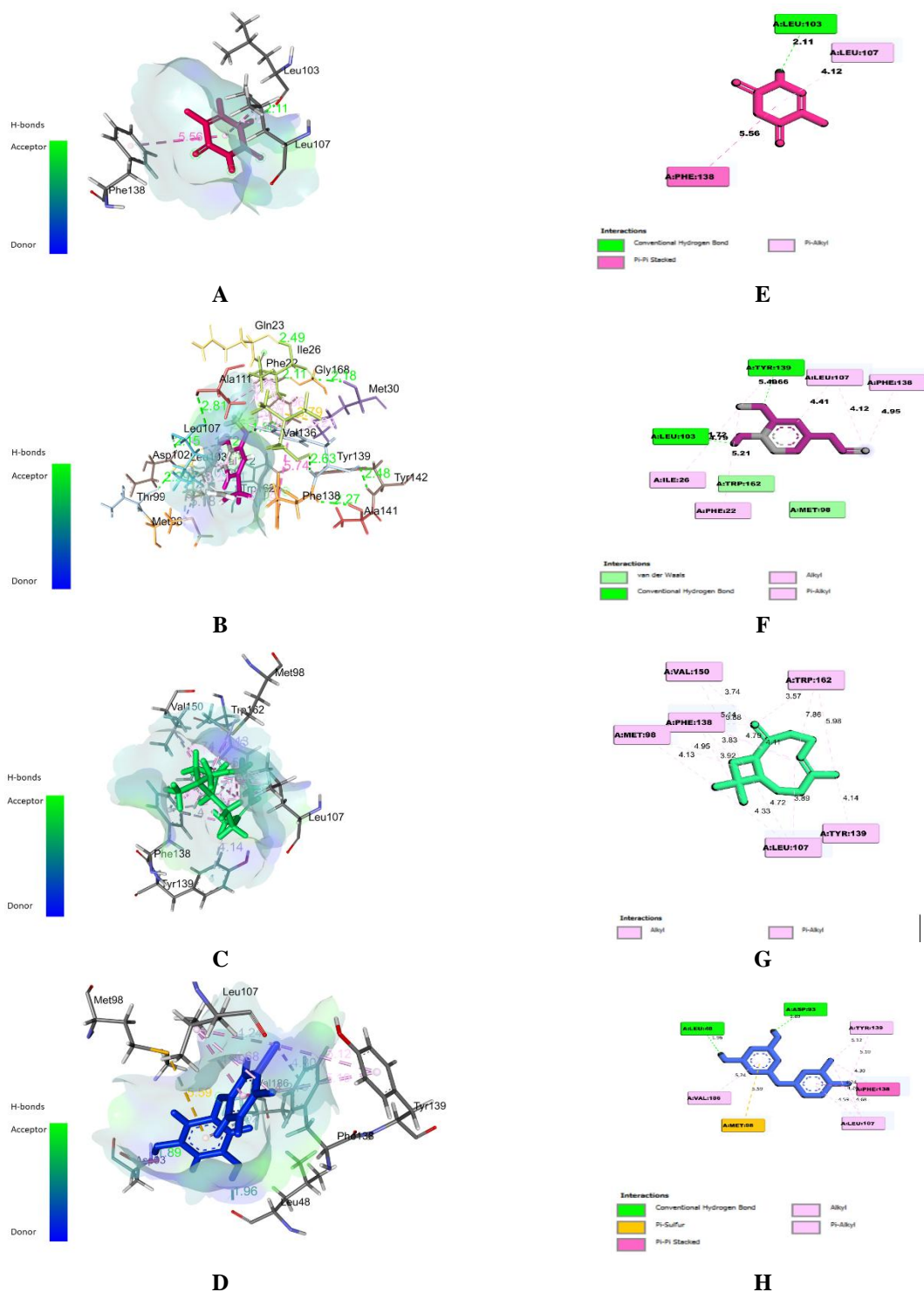


Figure 4 Protein-Ligand interaction poses of colorectal cancer target HSP90AA1 with compounds (A) A 3D docked interaction based on hydrogen bond acceptor (HBA) and donor (HBD) of 5- fluorouracil (5-FU), (B) eugenol (EUG), (C) beta-caryophyllene (BCP), (D) positive control (PC): 5-(3,4-dichloro-phenoxy)-benzene-1,3-diol inhibitor, (E) A 2D docked interaction of eugenol (EUG), (F) beta-caryophyllene (BCP), (G) 5- fluorouracil (5-FU), (H) positive control (PC): 5-(3,4-dichloro-phenoxy)-benzene-1,3-diol inhibitor at active domain of Heat shock protein 90- alpha (HSP90AA1) protein with interacting amino acids and H-bonds

control and test compounds was in four proteins, which include Heat Shock Protein- 90 alpha (HSP90AA1), Insulin-like Growth Factor 1 Receptor (IGF-1R), estrogen receptor (ESR1), and Caspase- 3 (CASP3). Figure 4 shows the docked poses of interactions in H-bond donor and acceptor form in 3D, bond length, and interacted amino acid residues in 2D of HSP90AA1 protein with test compounds. Over the last two decades, HSP90 has emerged as an intriguing target in the war on cancer. HSP90 interacts and supports numerous proteins that promote oncogenesis, thus distinguishing Hsp90 as a cancer enabler as it is regarded as essential for malignant transformation and progression (Zuehlke et al. 2015). The binding energy of 5-FU, EUG, BCP and 5-(3,4-dichloro-phenoxy)-benzene-1,3-diol inhibitor (positive control) for HSP90AA1 was -5.097,-7.515,-7.539 and -7.853 Kcal/mol respectively, which shows that eugenol and beta-caryophyllene can bind strongly with HSP90AA1 protein than the standard drug 5-Fluorouracil as shown in figure 4. A study done by Absalan and his co-workers proved that eugenol can positively interact with this small chaperone molecule of HSP90AA1 that may affect stem cell aging via telomere or telomerase-dependent pathway (Absalan et al. 2017). In addition to their findings, we found out that eugenol can bind more effectively with the hub proteins such as HSP90AA1, ESR1, CASP3, and IGF-1R than any other selected compounds. HSP90 targets multiple signaling pathways by disrupting metastatic proteins, thus inhibiting epithelial to mesenchymal transition in cancer cells (Zhang et al. 2021; Anwar et al. 2022). Type-I insulin-like growth factor receptor is a tyrosine kinase receptor that is over-expressed in many cancer processes, such as cell growth, cell proliferation, cell differentiation, apoptosis, and angiogenesis. Moreover, it is involved in PI3K-AKT and MAPK signaling pathways (Codony-Servat et al. 2017). The other key target was estrogen receptor type 1 (ESR1) is a cell cycle regulator protein that further interacts with PI3K, AKT, ERK, MAPK, and NF-KB proteins for anti-apoptosis mechanism (Williams et al. 2016; Ditunno et al. 2021). Increased Caspase 3 (CASP3) causes apoptosis, and its activation is a positive indicator of cancer treatment (Zou and Xu 2018). Eugenol exerts its apoptosis-inducing effects by cleaving caspase 3, with a significant increase in its active form showing apoptosis-inducing properties (Fathy et al. 2019), which also limits the cells' ability to metastasize and proliferate in the rise in ROS and cytochrome C's release (Abdullah et al. 2018; Anwar et al. 2022). Beta-caryophyllene also induces apoptosis in mouse blood cancer cell lines through caspase 3 induction (Amiel et al. 2012) and by downregulating PI3K/AKT/mTOR/S6K1 pathways and ROS-mediated MAPKs activation (Park et al. 2011; Dahham et al. 2015). All these four hub proteins (HSP90AA1, IGF-1R, ESR1, and CASP3) affect other proteins in downstream mechanisms in a way that inhibits cancer cell proliferation, induces apoptosis, and thus provides anticancer and anti-

metastatic properties. Targeting any of these proteins for therapeutic use in colorectal cancer treatment by our natural compounds alone or combined with chemotherapeutic drugs can be helpful in colorectal cancer treatment.

### Conclusion

In a multitarget strategy, if we combine the treatment of a drug with a phytochemical, it can target multiple proteins to exert their effects as anticancer agents. The synergism proved effective against colorectal cancer *in-silico* and *in-vitro* when 5-FU was combined with EUG and BCP. These natural compounds effectively reduced IC<sub>50</sub> value in combination with conventional chemotherapeutic drugs. They can target HSP90AA1 as a key protein to further provide anti-metastatic effect in colorectal cancer treatment through which it can promote autophagy and inhibit apoptosis through PI3K/Akt/mTOR pathway and JNK/P38 pathway, which are key pathways in epithelial to mesenchymal transition inhibition.

### Abbreviations

CRC: Colorectal Cancer; EUG: Eugenol; BCP: Beta-Caryophyllene; 5-FU: 5-fluorouracil; TNBC: Triple Negative Breast Cancer; HER2 Human epidermal growth receptor 2; MMP: Matrix Metalloproteinase; TGFβ: Tumour Growth Factor beta; PI3K-Akt: The Phosphatidylinositol 3-kinase/ Protein kinase B; MAPK: Mitogen-activated protein kinase; MTT: 3-(4,5-dimethylthiazol-2-yl)-2, 5-diphenyltetrazolium bromide; Fa-CI: Fraction Affected-Combination Index; ADME: absorption, distribution, metabolism, and excretion; BBB: Blood-Brain Barrier; PPB: Plasma Protein Binding; HIA: Human Intestinal Absorption; P-gp: p-glycoproteins; SDF: Structure Data File; SMILES: Simplified molecular input line entry system; STITCH: Search Tool for Interacting Chemicals; PPI: Protein- Protein Interaction; C-D-T: Compound-Disease-Target; DAVID: The Database for Annotation, Visualization, and Integration Discovery; GO: Gene Ontology; KEGG: Kyoto Encyclopaedia of Genes and Genomes; FDR: False Discovery Rate; BP: Biological Processes; CC: Cellular Compounds; MF: Molecular Functions; MDDR: MDL Drug Data Report; RMSD: Root mean square deviation

### Conflict of Interest

The authors have no conflicts of interest to declare relevant to this article's content.

### Acknowledgments

The authors acknowledge the Department of Chemistry for providing the facility and access to the computational software.

### Funding

This work was supported by SHODH – ScHeme Of Developing High quality research, Knowledge Consortium of Gujarat, Education Department, Government of Gujarat with Student Ref No: 201901380008 (KCG/SHODH/2020-21/).

### Author contributions (CREDIT)

D.J. (Devendrasinh Jhala) – Conceptualization, methodology, experimental studies, formal analysis, investigation, resources, funding acquisition, manuscript review and editing; K.T. (Krupali Trivedi) – Conceptualization, software, methodology, experimental studies, data curation, data analysis, writing- original draft preparation, manuscript review and editing, funding acquisition; P.R., N.P., S.P., B.G. – Conceptualization, software, validation, data analysis, manuscript review; S.C., A.P. – Manuscript review, resources, investigation, supervision. All authors have read and agreed to the publication of the manuscript.

### References

- Abdullah, M.L., Al-Shabanah, O., Hassan, Z.K., & Hafez, M.M. (2021). Eugenol-Induced Autophagy and Apoptosis in Breast Cancer Cells via PI3K/AKT/FOXO3a Pathway Inhibition. *International Journal of Molecular Sciences*, 22(17), 9243.
- Abdullah, M.L., Hafez, M.M., Al-Hoshani, A., & Al-Shabanah, O. (2018) Anti-metastatic and antiproliferative activity of eugenol against triple negative and HER2 positive breast cancer cells. *BMC Complementary and Alternative Medicine*, 18(1), 1-11.
- Absalan, A., Mesbah-Namin, S.A., Tiraihi, T., & Taheri, T. (2017). Cinnamaldehyde and eugenol change the expression folds of AKT1 and DKC1 genes and decrease the telomere length of human adipose-derived stem cells (hASCs): An experimental and *in silico* study. *Iranian Journal of Basic Medical Sciences*, 20(3), 316–26.
- Ahmed, E.A., Abu Zahra, H., Ammar, R.B., Mohamed, M.E., & Ibrahim, H.I.M. (2022). Beta-Caryophyllene Enhances the Anti-Tumor Activity of Cisplatin in Lung Cancer Cell Lines through Regulating Cell Cycle and Apoptosis Signaling. *Molecules*, 27(23), 8354.
- Alonso Gómez, C., Satta, V., Díez Gutiérrez, P., Fernández Ruiz, J., & Sagredo Ezquioga, O. (2022). Preclinical investigation of  $\beta$ -caryophyllene as a therapeutic agent in an experimental murine model of Dravet syndrome. *Neuropharmacology*, 205, 108914.
- Amiel, E., Ofir, R., Dudai, N., Soloway, E., Rabinsky, T., & Rachmilevitch, S. (2012).  $\beta$ -Caryophyllene, a compound isolated from the biblical balm of gilead (*Commiphora gileadensis*), is a selective apoptosis inducer for tumor cell lines. *Evidence-Based Complementary and Alternative Medicine*, 2012. <https://doi.org/10.1155/2012/872394>
- Amin, M.L. (2013). P-glycoprotein Inhibition for Optimal Drug Delivery. *Drug Target Insights*, 7, DTI-S12519.
- Anwar, S., Malik, J.A., Ahmed, S., Kameshwar, V.A., Alanazi, J., Alamri, A., & Ahemad, N. (2022). Can Natural Products Targeting EMT Serve as the Future Anticancer Therapeutics? *Molecules*, 27(22), 7668.
- Arnold, M., Sierra, M.S., Laversanne, M., Soerjomataram, I., Jemal, A., & Bray, F. (2017). Global patterns and trends in colorectal cancer incidence and mortality. *Gut*, 66 (4), 683–91.
- Assenov, Y., Ramírez, F., Schelhorn, S.E., Lengauer, T., & Albrecht, M. (2008). Computing topological parameters of biological networks. *Bioinformatics*, 24(2), 282–4. <https://doi.org/10.1093/bioinformatics/btm554>
- Benarba, B., & Pandiella, A. (2018). Colorectal cancer and medicinal plants: Principle findings from recent studies. *Biomedicine & Pharmacotherapy*, 107, 408–423.
- Bhardwaj, P., & Dilbaghi, N. (2022). Pharmaceutical Nanoarchitectonics: Molecular Pharmaceutics and Smart Delivery of  $\beta$ -Caryophyllene Constellated 5-FU Nanoinvasomes for Skin Cancer Therapy. *BioNanoScience*, 12(4), 1329–40.
- Casale, J., & Patel, P. (2022). Fluorouracil. StatPearls, *Treasure Island (FL)*. <http://www.ncbi.nlm.nih.gov/books/NBK549808/>
- Chou, T.C., & Talalay, P. (1984). Quantitative analysis of dose-effect relationships: the combined effects of multiple drugs or enzyme inhibitors. *Advances in Enzyme Regulation*, 22, 27–55. [https://doi.org/10.1016/0065-2571\(84\)90007-4](https://doi.org/10.1016/0065-2571(84)90007-4)
- Codony-Servat, J., Cuatrecasas, M., Asensio, E., Montironi, C., Martinez-Cardus, A., Marin-Aguilera, M., & Maurel, J. (2017). Nuclear IGF-1R predicts chemotherapy and targeted therapy resistance in metastatic colorectal cancer. *British Journal of Cancer*, 117, 1777–1786. <https://doi.org/10.1038/bjc.2017.279>
- Dahham, S.S., Tabana, Y.M., Iqbal, M.A., Ahamed, M. B., Ezzat, M. O., Majid, A. S., & Majid, A. M. (2015). The Anticancer, Antioxidant and Antimicrobial Properties of the Sesquiterpene  $\beta$ -Caryophyllene from the Essential Oil of *Aquilaria crassna*. *Molecules*, 20, 11808–11829. <https://doi.org/10.3390/molecules200711808>
- das Chagas Pereira de Andrade, F., & Mendes, A.N. (2020). Computational analysis of eugenol inhibitory activity in

- lipoxygenase and cyclooxygenase pathways. *Scientific Reports*, *10*(1), 1–14.
- Deepak, V., Kasonga, A., Kruger, M.C., & Coetzee, M. (2015). Inhibitory effects of eugenol on RANKL-induced osteoclast formation via attenuation of NF- $\kappa$ B and MAPK pathways. *Connective Tissue Research*, *56*, 195–203. <https://doi.org/10.3109/03008207.2014.989320>
- Di, L. (2017). Reaction phenotyping to assess victim drug-drug interaction risks. *Expert Opinion on Drug Discovery*, *12*, 1105–1115. <https://doi.org/10.1080/17460441.2017.1367280>
- Ditunno, I., Losurdo, G., Rendina, M., Pricci, M., Girardi, B., Ierardi, E., & Di Leo, A. (2021). Estrogen Receptors in Colorectal Cancer: Facts, Novelties and Perspectives. *Current Oncology*, *28*, 4256–4263. <https://doi.org/10.3390/curroncol28060361>
- Fan, Q., Guo, L., Guan, J., Chen, J., Fan, Y., Chen, Z., & Li, H. (2020). Network Pharmacology-Based Study on the Mechanism of Gegen Qinlian Decoction against Colorectal Cancer. *Evidence Based Complementary Alternative Medicine*, *2020*, 1–14. <https://doi.org/10.1155/2020/8897879>
- Fathy, M., Fawzy, M.A., Hintzsche, H., Nikaido, T., Dandekar, T., & Othman, E. M. (2019). Eugenol Exerts Apoptotic Effect and Modulates the Sensitivity of HeLa Cells to Cisplatin and Radiation. *Molecules*, *24*, 3979. <https://doi.org/10.3390/molecules24213979>
- Fernández-Ruiz, J., Sagredo, O., Pazos, M.R., Garcia, C., Pertwee, R., Mechoulam, R., & Martínez-Orgado, J. (2013). Cannabidiol for neurodegenerative disorders: important new clinical applications for this phytocannabinoid? *British Journal of Clinical Pharmacology*, *75*, 323–333. <https://doi.org/10.1111/j.1365-2125.2012.04341.x>
- Garrido, A., Lepailleur, A., Mignani, S.M., Dallemagne, P., & Rochais, C. (2020). hERG toxicity assessment: Useful guidelines for drug design. *European Journal of Medicinal Chemistry*, *195*, 112290. <https://doi.org/10.1016/j.ejmech.2020.112290>
- Gibbs, J.P., Hyland, R., & Youdim, K. (2006). Minimizing Polymorphic Metabolism in Drug Discovery: Evaluation of the Utility of in Vitro Methods for Predicting Pharmacokinetic Consequences Associated with CYP2D6 Metabolism. *Drug Metabolism and Disposition*, *34*, 1516–1522. <https://doi.org/10.1124/dmd.105.008714>
- Gonzalez, E., Jain, S., Shah, P., Torimoto-Katori, N., Zakharov, A., Nguyen, D. T., & Xu, X. (2021). Development of Robust Quantitative Structure-Activity Relationship Models for CYP2C9, CYP2D6, and CYP3A4 Catalysis and Inhibition. *Drug Metabolism and Disposition*, *49*, 822–832. <https://doi.org/10.1124/dmd.120.000320>
- Halgren, T.A., Murphy, R.B., Friesner, R.A., Beard, H. S., Frye, L. L., Pollard, W. T., & Banks, J. L. (2004). Glide: A New Approach for Rapid, Accurate Docking and Scoring. 2. Enrichment Factors in Database Screening. *Journal of Medicinal Chemistry*, *47*, 1750–1759. <https://doi.org/10.1021/jm030644s>
- Hemaiswarya, S., & Doble, M. (2013). Combination of phenylpropanoids with 5-fluorouracil as anticancer agents against human cervical cancer (HeLa) cell line. *Phytomedicine*, *20*, 151–158. <https://doi.org/10.1016/j.phymed.2012.10.009>
- Huang, S., Zhang, Z., Li, W., Kong, F., Yi, P., Huang, J., & Zhuang, S. (2020). Network Pharmacology-Based Prediction and Verification of the Active Ingredients and Potential Targets of Zuojinwan for Treating Colorectal Cancer. *Drug Design, Development and Therapy*, *14*, 2725–2740. <https://doi.org/10.2147/DDDT.S250991>
- Jubeen, F., Ijaz, S., Jabeen, I., Aftab, U., Mehdi, W., Altaf, A., & Iqbal, M. (2022). Anticancer potential of novel 5-Fluorouracil co-crystals against MCF7 breast and SW480 colon cancer cell lines along with docking studies. *Arabian Journal of Chemistry*, *15*, 104299. <https://doi.org/10.1016/j.arabj.2022.104299>
- Kadoyama, K., Miki, I., Tamura, T., Brown, J. B., Sakaeda, T., & Okuno, Y. (2011). Adverse Event Profiles of 5-Fluorouracil and Capecitabine: Data Mining of the Public Version of the FDA Adverse Event Reporting System, AERS, and Reproducibility of Clinical Observations. *International Journal of Medicinal Sciences*, *9*, 33–39. <https://doi.org/10.7150/ijms.9.33>
- Kamal, M.M., Akter, S., Lin, C.N., & Nazzal, S. (2020). Sulforaphane as an anticancer molecule: mechanisms of action, synergistic effects, enhancement of drug safety, and delivery systems. *Archives of Pharmacal Research*, *43*, 371–384. <https://doi.org/10.1007/s12272-020-01225-2>
- Li Z, Veeraraghavan, V. P., Mohan, S. K., Bolla, S. R., Lakshmanan, H., Kumaran, S., & Chinnathambi, A. (2020). Apoptotic induction and anti-metastatic activity of eugenol encapsulated chitosan nanopolymer on rat glioma C6 cells via alleviating the MMP signaling pathway. *Journal of Photochemistry and Photobiology B: Biology*, *203*, 111773. <https://doi.org/10.1016/j.jphotobiol.2019.111773>
- Lipinski, C.A., Lombardo, F., Dominy, B.W., & Feeney, P.J. (1997). Experimental and computational approaches to estimate solubility and permeability in drug discovery and development settings. *Advanced Drug Delivery Reviews*, *64*, 4–17. [https://doi.org/10.1016/S0169-409X\(96\)00423-1](https://doi.org/10.1016/S0169-409X(96)00423-1)

- Mosmann, T. (1983). Rapid colorimetric assay for cellular growth and survival: Application to proliferation and cytotoxicity assays. *Journal of Immunological Methods*, 65, 55–63. [https://doi.org/10.1016/0022-1759\(83\)90303-4](https://doi.org/10.1016/0022-1759(83)90303-4)
- Naren, G., Guo, J., Bai, Q., Fan, N., & Nashun, B. (2022). Reproductive and developmental toxicities of 5-fluorouracil in model organisms and humans. *Expert Reviews in Molecular Medicine*, 24, e9. <https://doi.org/10.1017/erm.2022.3>
- Ng, P.L., Rajab, N.F., Then, S.M., Mohd Yusof, Y. A., Wan Ngah, W. Z., Pin, K. Y., & Looi, M. L. (2014). Piper betle leaf extract enhances the cytotoxicity effect of 5-fluorouracil in inhibiting the growth of HT29 and HCT116 colon cancer cells. *Journal of Zhejiang University-Science B*, 15, 692–700. <https://doi.org/10.1631/jzus.B1300303>
- Noor, F., Tahir ul Qamar, M., Ashfaq, U.A., Albutti, A., Alwashmi, A. S., & Aliasir, M. A. (2022). Network Pharmacology Approach for Medicinal Plants: Review and Assessment. *Pharmaceuticals*, 15, 572. <https://doi.org/10.3390/ph15050572>
- Park, K.R., Nam, D., Yun, H.M., Lee, S. G., Jang, H. J., et al. (2011).  $\beta$ -Caryophyllene oxide inhibits growth and induces apoptosis through the suppression of PI3K/AKT/mTOR/S6K1 pathways and ROS-mediated MAPKs activation. *Cancer Letters*, 312, 178–188. <https://doi.org/10.1016/j.canlet.2011.08.001>
- Prival, M.J., & Zeiger, E. (1998). Chemicals mutagenic in *Salmonella typhimurium* strain TA1535 but not in TA100. *Mutation Research/Genetic Toxicology and Environmental Mutagenesis*, 412, 251–260. [https://doi.org/10.1016/S1383-5718\(97\)00196-4](https://doi.org/10.1016/S1383-5718(97)00196-4)
- Sheridan, R.P., & Shpungin, J. (2004). Calculating Similarities between Biological Activities in the MDL Drug Data Report Database. *Journal of Chemical Information and Computer Sciences*, 44, 727–740. <https://doi.org/10.1021/ci034245h>
- Surducun, D.A., Racea, R.C., Cabuta, M., Olariu, I., Macasoi, I., Rusu, L. C., & Pricop, M. O. (2023). Eugenol Induces Apoptosis in Tongue Squamous Carcinoma Cells by Mediating the Expression of Bcl-2 Family. *Life*, 13, 22. <https://doi.org/10.3390/life13010022>
- Toiyama, Y., Hur, K., Tanaka, K., Inoue, Y., Kusunoki, M., Boland, C. R., & Goel, A. (2014). Serum miR-200c Is a Novel Prognostic and Metastasis-Predictive Biomarker in Patients With Colorectal Cancer. *Annals of Surgery*, 259, 735–743. <https://doi.org/10.1097/SLA.0b013e3182a6909d>
- Ulanowska, M., & Olas, B., (2021). Biological Properties and Prospects for the Application of Eugenol—A Review. *International Journal of Molecular Sciences*, 22, 3671. <https://doi.org/10.3390/ijms22073671>
- Veber, D.F., Johnson, S.R., Cheng, H-Y., Smith, B. R., Ward, K. W., & Kopple, K. D. (2002). Molecular properties that influence the oral bioavailability of drug candidates. *Journal of Medicinal Chemistry*, 45, 2615–2623
- Williams, C., DiLeo, A., Niv, Y., & Gustafsson, J.Å. (2016). Estrogen receptor beta as target for colorectal cancer prevention. *Cancer Letters*, 372, 48–56. <https://doi.org/10.1016/j.canlet.2015.12.009>
- Zhang, A., Qi, X., Du, F., Zhang, G., Li, D., & Li, J. (2021). PNSA, a Novel C-Terminal Inhibitor of HSP90, Reverses Epithelial–Mesenchymal Transition and Suppresses Metastasis of Breast Cancer Cells In Vitro. *Marine Drugs*, 19, 117. <https://doi.org/10.3390/md19020117>
- Zhu, H., Hao, J., Niu, Y., Liu, D., Chen, D., & Wu, X. (2018). Molecular targets of Chinese herbs: a clinical study of metastatic colorectal cancer based on network pharmacology. *Scientific Reports*, 8, 7238. <https://doi.org/10.1038/s41598-018-25500-x>
- Zou, W.W., & Xu, S.P. (2018). Galangin inhibits the cell progression and induces cell apoptosis through activating PTEN and Caspase-3 pathways in retinoblastoma. *Biomedicine & Pharmacotherapy*, 97, 851–863. <https://doi.org/10.1016/j.biopha.2017.09.144>
- Zuehlke, A.D., Beebe, K., Neckers, L., & Prince, T. (2015). Regulation and function of the human HSP90AA1 gene. *Gene*, 570, 8–16. <https://doi.org/10.1016/j.gene.2015.06.018>